The new digital orthometric elevation model of Kilimanjaro

Pascal Sirguey
National School of Surveying
University of Otago
Dunedin, New Zealand
pascal.sirguey@otago.ac.nz

Nicolas J. Cullen
Geography Department
University of Otago
Dunedin, New Zealand
nicolas.cullen@otago.ac.nz

Jorge Filipe Dos Santos
Vale Technological Institute
Brazil
jorge.filipe@itv.org

Abstract

Kibo, the highest of three peaks of Kilimanjaro, has not benefited from a medium to large scape topographic mapping in about 50 years. The rapidly changing topography associated with the glacier retreat and the fact that the slopes of Kibo attract about 40,000 climbers each year thus justify the need to develop a new topographic survey of this outstanding landmark, designated a UNESCO World Heritage Site in 1987. In this context, the application of the photogrammetric principles to the latest generation of very high resolution space-borne optical sensors (VHRS) offers new surveying opportunities by enabling the topographic mapping of remote and hardly accessible areas at large scale with unprecedented spatial resolution. This paper illustrates the potential of a space-borne photogrammetric survey technique by reporting on the last effort to map the topography of Kibo from GeoEye-1 stereo imagery, which has led to the creation of a new 50cm resolution Digital Elevation Model (DEM), namely KILISoSDEM2012. Furthermore, this new model is combined with the refined local geoid model KILI2008 generated from gravimetric observations captured by the international team that completed the last survey of the orthometric height of Kibo in October 2008. This paper shows that the new digital orthometric elevation model exhibits a 35% and 25% improvement in planimetric and elevation accuracy, respectively, compared to the specifications of GeoEye-1 Precision products.

1 Introduction

In 1912, German explorer Eduard Oehler and glaciologist Fritz Klute completed the first topographic survey of Kibo, the highest of three peaks of Kilimanjaro, using the emerging photogrammetric technique (Klute, 1920, 1921). This led to a 1:50,000 scale map being produced, the quality of which should be praised given the complexity of the terrain and the technical limitations of the emerging surveying technique at the time.

The mapping of Kilimanjaro at a scale of 1:50,000 was not repeated for another 50 years. A photogrammetric survey was conducted in January 1962 for the main mountain, following a survey in March 1958 for its surroundings (Directorate of Overseas Surveys, 1964; Young and Hastenrath, 1987; Shirima, 2013). Although more recent

In: S. Winter and C. Rizos (Eds.): Research@Locate'14, Canberra, Australia, 07-09 April 2014, published at http://ceur-ws.org

research projects have used some limited survey data in selected areas of the volcano, such as to characterise the demise of glaciers on Kibo (Cullen et al., 2013), the massive volcano has not benefited from an updated and more detailed survey in 50 years. The rapidly changing topography associated with the glacier retreat and the fact that the slopes of Kibo attract about 40,000 climbers each year (International Mountaineering and Climbing Federation, UIAA, 2013) justify the need to develop a new topographic survey of this outstanding landmark, designated a UNESCO World Heritage Site in 1987.

In this context, the application of the photogrammetric principles to the latest generation of very high resolution space-borne optical sensors (VHRS) offers new surveying opportunities by enabling the topographic mapping of remote and hardly accessible areas at large scale with unprecedented spatial resolution. Recent hardware and software advances now allow dense point clouds to be generated, thus making the use of VHRS stereo imagery a viable technique to complete a large topographic survey at a small pecuniary and logistical cost. Thus, 100 years after Klute and Oehler completed the first ground based photogrammetric survey of Kibo, and 50 years after the most recent aerial photogrammetric survey, this paper illustrates the potential of a spaceborne photogrammetric survey technique by reporting on the last effort to map the topography of Kibo from GeoEye-1 stereo imagery. This has led to the creation of a new 50cm resolution Digital Elevation Model (DEM), namely KILISoSDEM2012. Furthermore, orthometric heights are obtained by combining this new DEM with the refined local geoid model KILI2008 generated from gravimetric observations captured by the international team that completed the last survey of the orthometric height of Kibo in October 2008 (KILI2008, 2009).

2 Data and methods

2.1 Satellite imagery

The GeoEye-1 sensor belongs to the latest generation of very high spatial resolution optical sensors on the civil market. It was launched on 6 September 2008 by GeoEye Inc (now merged with Digital Globe) and supports the capture of imagery at 1.65 m in four multispectral bands (MSI, visible and near infrared) and 0.41 m in the panchromatic band (PAN) although data is sold at 2 m and 50 cm resolution due to US government regulation. A GeoStereo product was ordered over an area of about 100 km2 centred on Reusch Crater (see Figure 1). Because of the persistent cloud cover on Kibo, the minimum cloud-free requirement could not be met despite the multiple acquisition attempts. This led to the acquisition and delivery of five bundle multispectral (MSI) and panchromatic (PAN) stereo pairs that, when considered together, provided almost a cloud-free coverage of the entire area (Table 1). Only two areas remained obscured in all pairs, namely north-west of the Great West Breach (a.k.a. Western Breach) and south-west of the Breach Wall (see Figure 1). In order to provide terrain elevation data for those gaps, a 15 m resolution Level 1A stereo image of the area, which had been acquired on 19 August 2004, was obtained from the Advanced Space-borne Thermal Emission and Reflection Radiometer (ASTER).

Table 1: Specifications of ASTER and GeoEye-1 imagery.

Date of each stereo pair (GMT)	Pixel size [m]	Cloud [%]	View Azim.	View Elev.
19 Aug 2004, 7:54	15.0	0	270	81.4
07:55	15.0	0	186.5	32.9
20 Sep 2012, 7:58	0.50	25	226.6	74.3
07:57	0.50	30	354.5	61.6
9 Oct 2012, 07:49	0.50	65	33.8	61.3
07:50	0.50	52	147.1	74.1
20 Oct 2012, 07:50	0.50	59	33.8	64.4
07:51	0.50	54	155.8	73.3
23 Oct 2012, 07:59	0.50	68	345.7	61.6
08:00	0.50	57	258.2	75.5
24 Jan 2013, 07:48	0.50	22	68.7	71.8
07:49	0.50	23	156.7	64.4

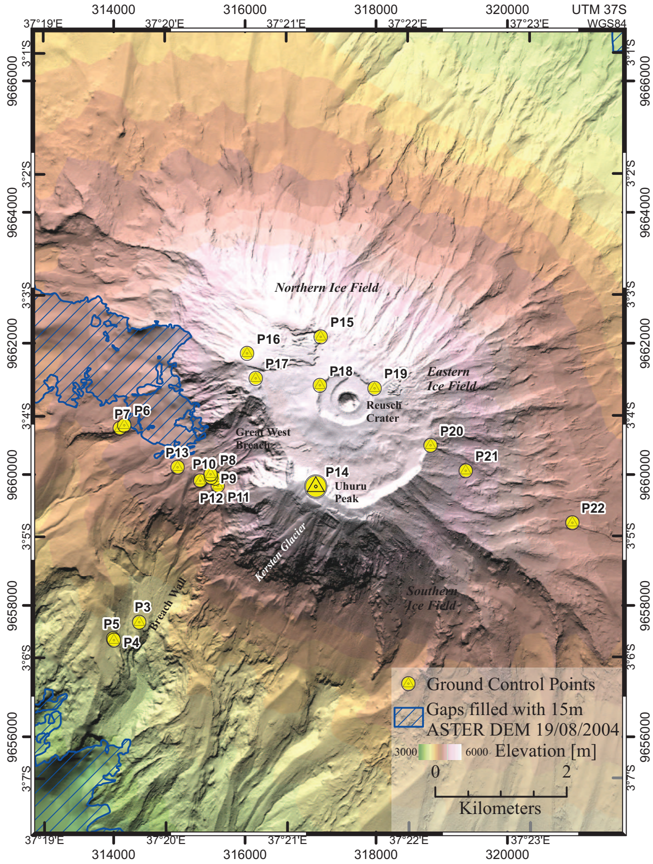

Figure 1: Colourized shaded relief of KILISoSDEM2012. Note the position of the 20 Ground Control Points used in the triangulation, as well as the areas with remaining obscuration by clouds in the GeoEye images that were filled with 15m resolution elevation points derived from an ASTER stereo image on 19/08/2004.

2.2 Ground control

Twenty Ground Control Points (GCPs) were collected on Kibo over 20-26 September 2012, thus matching or close to the capture dates. Ground features such as huts, a helicopter pad, prominent rocks, and well identified ice boundaries and ground discoloration marks were used. The WGS84 coordinates of these GCPs were measured using a Leica GS20 GPS L1 Code receiver in static mode with an occupation time of 2 minutes. The GPS data were post-processed via differential correction using the MAL2 IGS permanent GPS site located at Malindi, Kenya about 270 km away (great circle distance). Despite the relatively long baseline and short occupation time, post-processing yielded mean position quality measures RMS_{xy}=0.29 m and RMS_z=0.48 m. This was considered of suitable accuracy to support the triangulation of the 50 cm PAN stereo pairs.

2.3 Image block and triangulation

The triangulation of the satellite image stereo-pairs was conducted in ERDAS LPS 2013. A single image block based on the GeoEye-1 Rational Polynomial Coefficient (RPC) model was formed with the 10 panchromatic images corresponding to the five stereo-pairs. Processing the multi-date acquisition of GeoEye-1 images in a single block permitted a triangulation of all images together via a single bundle adjustment that enabled multiray photogrammetric processing. This allowed every pixel in numerous image overlaps to be processed, thus yielding redundancies that could be used to increase the accuracy of the point cloud via statistical filtering, or to increase the point density (Leberl et al., 2010).

About 300 tie points (TPs) were collected in a semi-automatic manner. Most TPs were automatically measured in LPS in multiple images and checked subsequently. The de-correlation between image pairs from different dates yielded a substantial amount of wrong points and points not being identified in all images. Those were remeasured manually when wrong, as well as transferred to images where they were not automatically identified. All twenty GCPs were converted to UTM37S cartographic projection, measured in all images where they appeared, and used as full control. Because of the uncertainties associated with the local geoid and the Tanzanian Vertical Datum (TVD) (see Saburi et al., 2000; KILI2008, 2009), heights above the reference WGS84 ellipsoid (HAE) were initially used. Any customized adjustments to other vertical datums could thus be easily processed subsequently to the triangulation and Digital Elevation Model production.

The ASTER stereo image was triangulated separately using the ASTER orbital pushbroom sensor model, 28 TPs, and 20 GCPs. Fifteen were GCPs collected during fieldwork that could be identified in the 15m ASTER images. Advantage was taken of the triangulated GeoEye image block to support the collection of five additional control points well distributed around Kibo with a sub-metre accuracy comparable to that of the GPS points.

2.4 DEM generation

The dense point cloud (PC) was generated with the enhanced Automatic Terrain Extraction (eATE) of LPS 2013 in a pseudo multiray approach. First, each of the four triangulated stereo pairs acquired in 2012 was considered separately to support most of the PC. The imagery acquired on 24 January 2013 was initially disregarded because of the substantially later and transient snow on ice surfaces. All 45 overlap combinations from all 10 images were then considered in order to generate more points in the non-glaciated stable areas with lower point density, such as those affected by repeated cloud obscuration or steep relief. The normalized cross correlation feature matching method was used with a relatively low threshold (0.65) and low contrast settings to generate numerous 3D points at the expense of a relatively large number of blunders (about 5%). The raw PC was generated in about one week with three parallel jobs on an Intel©i7-2600K equipped with 16 GB RAM; this yielded about 270 million points (MPts), with substantial redundancy in some areas.

The PC was thinned via median filtering within 50 cm grid cells, thus providing a first level of blunder removal. Further cleaning was achieved using a statistical outlier removal from the Point Cloud Library (PCL) (Rusu and Cousins, 2011), while remaining blunders were deleted via manual editing. Similarly, a PC was generated from the ASTER stereo pair from which about 13,000 points were used to fill gaps in the GeoEye PC. The cleaned gap-filled PC accounted for about 181 MPts at typically 50 cm spacing, meaning that more than 40% of the final 50 cm resolution raster DEM (437 Mcells) was supported by measured 3D points. Finally, the meshed PC was smoothed using a Laplacian operator and the resulting PC was interpolated to a 50cm resolution raster DEM using the ANUDEM thin plate smoothing spline terrain interpolator in ArcGIS 10 (Hutchinson, 1989).

2.5 Local Geoid model KILI2008

2.5.1 Data acquisition

In October 2008 an international project called KILI2008, involving 19 researchers from institutions of six different countries, aimed at accurately measuring the orthometric height of Mount Kilimanjaro (KILI2008, 2009). The measurements involved the combined use of GNSS double frequency receivers (Trimble R8) and two gravimeters (Scintrex CG3-M and Scintrex CG5) illustrated in Figure 2 (a) and (b), respectively. The gravimetric observations were necessary to estimate a local geoid with sufficient accuracy to convert the ellipsoidal heights from GNSS observations to orthometric heights.

Ninety nine gravimetric and GNSS data were acquired over 10 days at locations approximately distributed in a grid centered on Kibo, depending on logistic constraints and existing routes (Figure 2). GNSS static observations of 30 to 45 minutes duration were collected together with the gravimetric measurements. Two GNSS reference stations located in Moshi and Himo were used for coordinate correction. Seven additional GPS points were acquired along the Manrangu route between 3200 meters height and the summit (Uhuru Peak).

2.5.2 Data processing

The KILI2008 geoid was calculated based on the gravimetric measurements using the Standard Residual Terrain Modeling strategy (Forsberg and Tscherning, 1981). The long wavelengths of the geoid undulation were determined using degree 0-360 of the Earth Gravitational Model 2008 (EGM2008) (Pavlis et al., 2012). The effect associated with the mass of the mountain was computed with Least Squares Collocation (see KILI2008, 2009, for more details) and using topographic information obtained from Shuttle Radar Topography Mission (SRTM) Digital Terrain Elevation Data (DTED) Level 1 (Farr et al., 2007). The calculated KILI 2008 geoid surface is

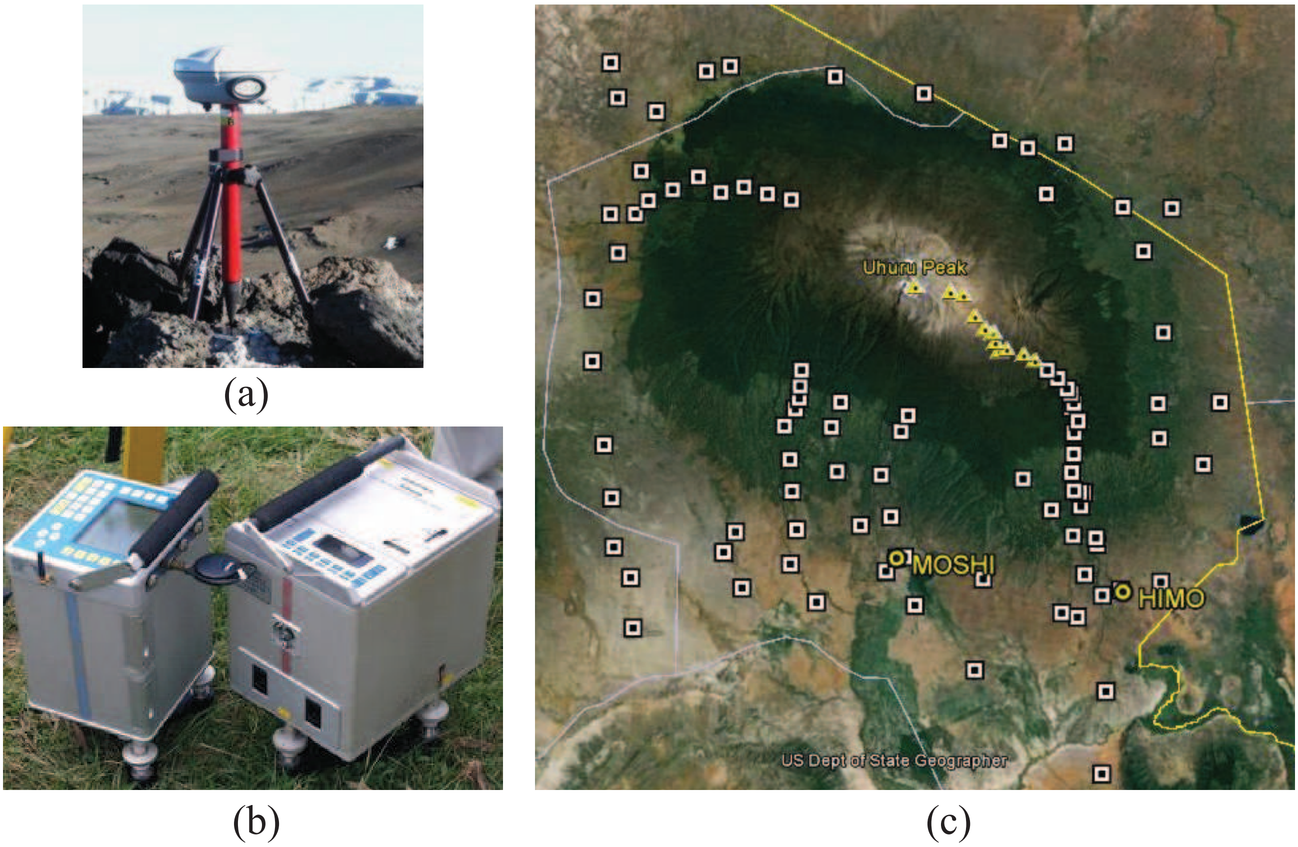

Figure 2: Instruments used during the KILI2008 project, namely (a) GNSS receiver Trimble R8 and (b) Scintrex CG3-M and Scintrex CG5 gravimeters. White squares in (c) indicate locations where both GNSS and gravimetric observations were collected, while only GNSS observations are identified as yellow triangles. GNSS reference stations are represented by yellow circles.

illustrated in Figure 3. Differences between KILI2008 and EGM2008 are -12 cm in Moshi, -12 cm in Himo and +21 cm at Uhuru Peak.

The GNSS data collected at the two reference stations were processed using the GIPSY-OASIS II software package in order to compute positions up to sub-centimeter level with respect to the ITRF2005 reference frame. Those two stations were later used as reference to compute the coordinates of the other points using Trimble Business Center.

The final orthometric heights obtained from the combination of GNSS survey and the KILI2008 geoid are referred to as global mean sea level elevation. A reference was needed to convert those heights to the national vertical datum of Tanzania. There was only one existing benchmark in the region with known height in that local datum situated close to Moshi. Using GNSS observations on that point it was possible to detect a 1.28 m offset between the global and the local vertical datum.

3 Results

3.1 Accuracy assessment

The triangulation results are shown in Table 2. Given the relatively small number of GCPs, the accuracy was independently assessed using a leave-one-out cross validation protocol (LOOCV), whereby each GCP was used as an independent check point in turn and the block re-triangulated. The residuals associated with each GCP were collected to quantify the quality of the triangulated block. The relative accuracy of the ASTER triangulation can be explained by the accurate collection of GCPs at a sub-pixel level being supported by the interpretation from the very high resolution GeoEye-1 triangulated image block. The consistency between the dependent and the independent LOOCV residuals further demonstrates the robustness of both triangulations.

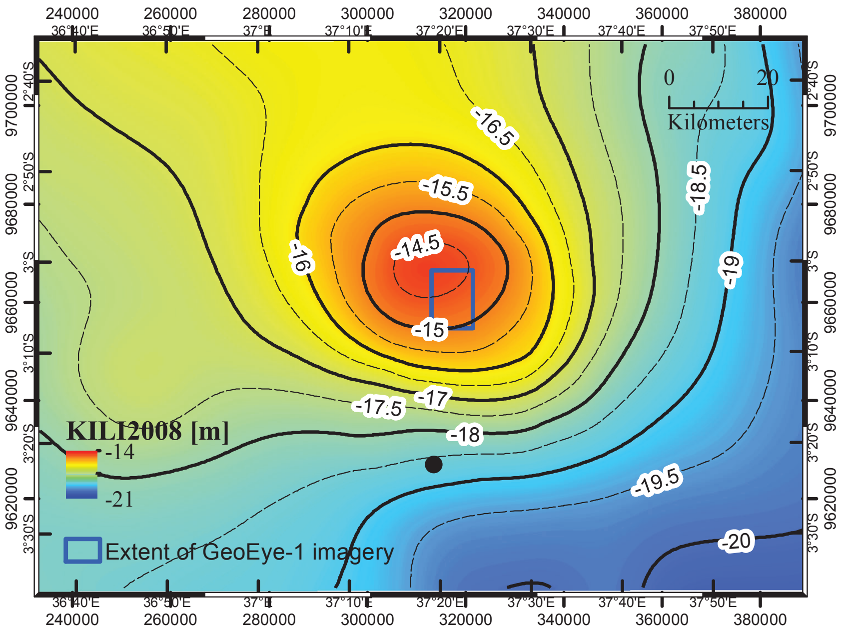

Figure 3: The KILI2008 geoid surface. The benchmark of the Tanzanian vertical datum is indicated by the black dot.

Table 2: Results of the image triangulation.

Image blocks	Pixel size [m]	Image RMSE [px]	Residuals of the control points [m]		
			RMS$_x$	RMS$_y$	RMS$_z$
GeoEye-1	0.50	0.27	0.42	0.61	1.09
Leave-one-out cross validation:			0.45	0.67	1.19
ASTER	15.0	0.21	1.92	1.89	4.40
Leave-one-out cross validation:			2.59	2.25	6.24

The propagation of Gaussian errors between the LOOCV residuals (Table 2) and the uncertainty of the GPS survey (Section 2.2) supports the accuracy specification of the final DEM product shown in Table 3. The latter exhibits a 35% and 25% improvement in planimetric and elevation accuracy, respectively, compared to the specifications of GeoEye-1 Precision products.

In Table 3, $RMSE = \sqrt{RMS_x + RMS_y}$ denotes the root mean square planimetric error. $CE90 = 1.5175 \times RMSE$ (Circular Error of 90%) is commonly used for quoting and validating geodetic image registration accuracy. A CE90 value is the minimum diameter of the horizontal circle that can be centred on all photo-identifiable Ground Control Points (GCPs) and also contain 90% of their respective twin counterparts acquired in an independent geodetic survey (FGDC, 1998, pg. 3-21). A Linear Error of 90% (LE90) is commonly used for quoting and validating DEMs. $LE90 = 1.6449 \times RMS_z$ (Linear Error of 90%) and represents the linear vertical distance that 90% of control points and their respective twin matching counterparts acquired in an independent geodetic survey should be found from each other (FGDC, 1998, pg. 3-21). $NMAS$ is the approximate map scale equivalencies based on the United States National Map Accuracy Standard and is defined as $1/NMAS = 1181 \times CE90$ (FGDC, 1998, pg. 3-21).

Table 3: Accuracy of the final DEM product.

RMSE [m	CE90 [m]	LE90 [m]	NMAS
0.86	1.31	2.12	1:1,600

3.2 Vertical datum

The photogrammetric block and subsequent DEM were produced initially in terms of height above the WGS84 ellipsoid: KILISoSDEM2012$_{\mathrm{HAEWGS84}}$. In order to obtain the orthometric DEM, the geoid undulation KILI2008 was resampled to 50 cm using cubic convolution interpolation. KILISoSDEM2012$_{\mathrm{KILI2008}}$ was then obtained by subtraction between the DEM in ellipsoidal height and the geoid separation as follows:

$$KILISoSDEM2012_{KILI2008} = KILISoSDEM2012_{HAEWGS84} - KILI2008. \tag{1}$$

The new KILISoSDEM2012$_{\mathrm{KILI2008}}$ is illustrated in Figure 1, while Figure 4 shows the current topography of Kersten glacier. Figure 5 illustrates the level of detail of the new DEM by comparing 3D scenes with corresponding photographs of the Northern and Eastern Ice Field.

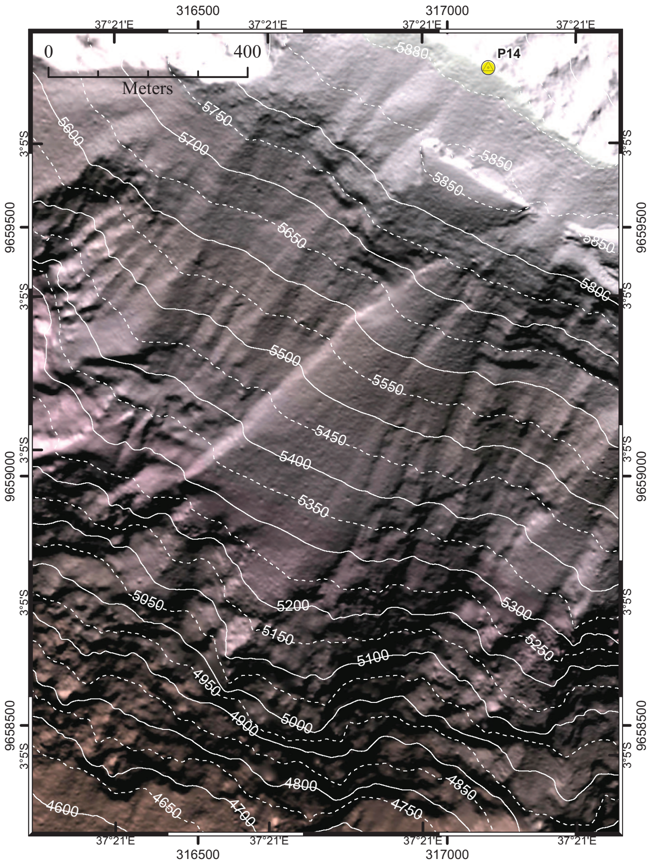

Figure 4: Colour shaded relief of KILISoSDEM2012 illustrating Kersten glacier. Contour lines indicate elevation in metres according to the Tanzanian Vertical Datum. Note the position of Uhuru peak at point P14.

3.3 About the height of Uhuru Peak

This study would not be complete without a note about the height of the highest point of Africa. The height of Uhuru Peak is most commonly known to be 5895 m amsl since the British Ordnance Survey in 1952 (Pugh, 1954). Before that, Klute (1921, ph. 149) reported on earlier estimates of what was named Kaiser Wilhelm Peak by

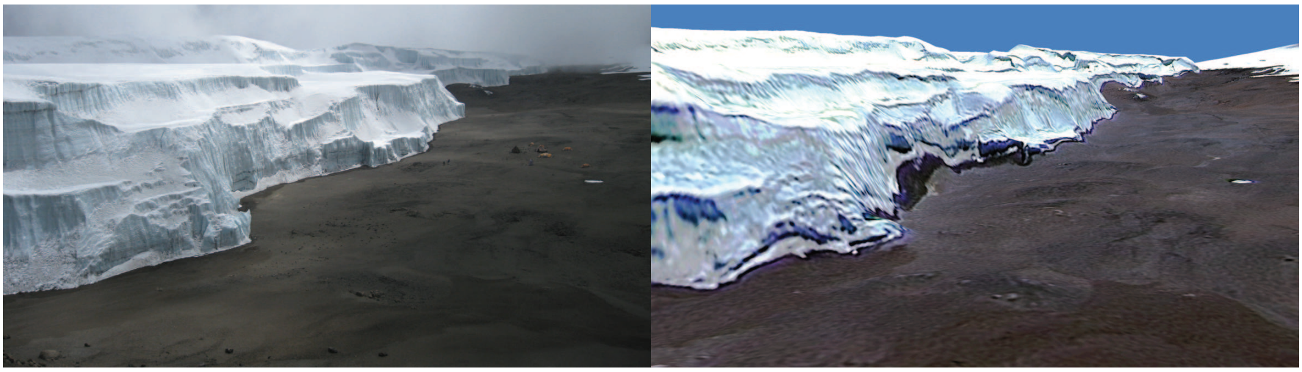

(a)

(b)

Figure 5: Left: Photo of (a) the Northern ice field seen from the top of the Western Breach approximately from P17 (Figure 2) eastward; (b) the Eastern ice field approximately from P19 location eastward (credit: Nicolas Cullen, 25 September 2012). Right: 3D visualisation of the KILISoSDEM2012 DEM at both corresponding locations: (a) GeoEye true-colour orthoimage of 20 September 2012 draped on the DEM; (b) shaded relief of the DEM.

Hans Meyer in 1889 (Meyer, 1891, pg. 154). Meyer estimated the height at 6010m using an aneroid barometer (Meyer, 1891, pg. 375-378). Klute (1921) also refers to the Anglo-German boundary expedition (1904-1906) which estimated Kibo to reach a height between 5888 and 5892 m although it is suspected that surveyors could not have seen the summit from their trigonometric point. Klute (1921) finally provided an estimated height of 5930 m from his photogrammetric survey Figure 1), although this figure is tarnished by the fact that the altitudes of the photogrammetric stations were determined on the basis of uncertain barometric measurements, rather than trigonometrically (Gillman, 1923).

In 1999, an accurate GPS survey was conducted at Uhuru Peak which led to a measured an ellipsoidal height of 5875.50 m (Saburi et al., 2000). This corresponded to the orthometric height which was estimated to be 5891.77 m based on the EGM96 geoid model that indicated a separation of -16.27 m at this location. Finally, a mean shift of 0.59 m was found with the Tanzanian height datum, thus yielding the final estimate of 5892.37 m. In 2008, the KILI2008 team (KILI2008, 2009) revised the geoid separation to be -14.48 m at Uhuru Peak. Given the ellipsoidal height of 5875.43 m (solution from the GIPSY software), the orthometric height above the KILI2008 geoid was found to be 5889.91 m $\pm$ 0.25 m. The additional departure from the TVD of 1.28 m at the Moshi benchmark yielded the most recent and assumedly most accurate estimate of the height of Uhuru Peak to be 5891.19 m 0.25 m.

A GPS point was collected at Uhuru Peak for this study yielding a relatively inaccurate ellipsoidal height of 5872.90 m. However, the triangulation of the GeoEye image block allowed this error to be partially mitigated as the precise targeting of the Kilimanjaro summit yielded a height of 5874.4 m, just one metre less than Team KILI2008, and within the specifications of the final product (see Section 3.1). However, the final HAE from the smoothed, interpolated KILISoSDEM2012 at Uhuru Peak (317082.1E; 9659820.4N) is found to be 5873.6 m $\pm$ 2.1 m, while the orthometric height above KILI2008 is 5888.1 $\pm$ 2.1 m assuming a 2σ error of 0.30 m in the KILI2008 undulation (KILI2008, 2009). KILISoSDEM2012 exhibits a relatively higher point at 317078.7E; 9659817.7N, HAE = 5874.2m $\pm$ 2.1 m, Orthometric height = 5888.7m$\pm$2.1m which is however not significantly higher given the uncertainty. The lower value can likely be attributed to the smoothing and interpolation process given the proximity of Uhuru peak to the edge of the crater rim.

4 Conclusion

This study documents KILISoSDEM2012$_{\text{KILI2008}}$, the new 50 cm resolution orthometric DEM of Kibo, the highest peak of Kilimanjaro. It is derived from multiray photogrammetry applied to five GeoEye-1 stereo pairs combined with the refined geoid model KILI2008. Triangulation results and independent accuracy assessment based on a leave-one-out cross validation protocol show that the KILISoSDEM2012 meets an accuracy level that is substantially better than that specified for the GeoEye Precision products. This product can therefore be used to create new topographic maps of this important landmark at much larger scales than what exist today. This new topography will also support the characterization of the rapid demise of glaciers on Kibo (e.g., Sirguey et al., 2013). Finally, this study provides a practical example of how space-borne sensors can now be used to support surveying applications with relatively strict accuracy requirements.

Acknowledgements

This research was funded by the National School of Surveying and the Department of Geography, University of Otago, New Zealand. ASTER images were obtained with support from the Global Land Ice Measurement from Space (GLIMS). The authors thank Stephen Shirima, principal land surveyor and assistant director of the mapping division at the Ministry of Lands, Housing and Human Settlements Development, Dar es Salaam, Tanzania, for his useful insight. We also thank the KILI2008 Team coordinated by Rui M. S. Fernandes, John Msemwa, and Machiel Bos. The two anonymous reviewers are also thanked for their constructive comments on the manuscript. This research would not have been possible without the support from the following Tanzanian authorities (COSTECH, KINAPA, TANAPA, TAWIRI).

References

Cullen, N. J., P. Sirguey, T. Mölg, G. Kaser, M. Winkler, and S. J. Fitzsimons (2013, March). A century of ice retreat on Kilimanjaro: the mapping reloaded. *The Cryosphere 7*(2), 419–431.

Directorate of Overseas Surveys (1964). *Kilimanjaro, East Africa 1:50,000 (Tanganyika).* D.O.S. 422, series Y742, sheet 56/2, Edition 1. Directorate of Overseas Surveys for the Tanganyika Government.

Farr, T. G., P. A. Rosen, E. Caro, R. Crippen, R. Duren, S. Hensley, M. Kobrick, M. Paller, E. Rodriguez, L. Roth, D. Seal, S. Shaffer, J. Shimada, J. Umland, M. Werner, M. Oskin, D. Burbank, and D. Alsdorf (2007, May). The shuttle radar topography mission. *Review of Geophysics 45*(2), RG2004–.

FGDC (1998). Part 3: National standard for spatial data accuracy. In *Geospatial Positioning Accuracy Standards*, Number FGDC-STD-007.3-1998 in Geospatial Positioning Accuracy Standards, pp. 28. Reston, Virginia: Federal Geographic Data Committee.

Forsberg, R. and C. C. Tscherning (1981, September). The use of height data in gravity field approximation by collocation. *Journal of Geophysical Research 86*(B9), 7843–7854.

Gillman, C. (1923, January). Dr. Klute's map of Kilimanjaro. *The Geographical Journal 61*(1), 70.

Hutchinson, M. F. (1989). A new procedure for gridding elevation and stream line data with automatic removal of spurious pits. *Journal of Hydrology 106*, 211–232.

International Mountaineering and Climbing Federation, UIAA (2013). Safety and success on kilimanjaro. retrieved from http://www.theuiaa.org/kilimanjaro.html on September 27, 2013.

KILI2008, T. (2009, 3-8 May). Precise determination of the oorthometric height of Mt. Kilimanjaro. In *Proceedings of FIG Working Week*, Eilat, Israel, pp. 11pp.

Klute, F. (1920). *Ergebnisse der Forschungen am Kilimandscharo, 1912.* Berlin: D. Reimer (E. Vohsen).

Klute, F. (1921). Die stereophotogrammetrishe aufnahme der hochregionen des kilimandscharo. *Zeitschrift der Gesselschaft Erdkunde zu Berlin 56*, 144–151.

Leberl, F., A. Irschara, T. Pock, P. Melxner, M. Gruber, S. Scholz, and A. Wlechert (2010, October). Point clouds: Lidar versus 3D vision. *Photogrammetric Engineering and Remote Sensing 76*(10), 1123–1134.

Meyer, H. (1891). *Across East African glaciers: an account of the first ascent of Kilimanjaro*. London, UK: George Philip & son. Translated from the German by E. H. S. Calder.

Pavlis, N. K., S. A. Holmes, S. C. Kenyon, and J. K. Factor (2012). The development and evaluation of the Earth Gravitational Model 2008 (EGM2008). *Journal of Geophysical Research 117*(B4), B04406–.

Pugh, K. T. (1954). *Height determination of Kilimanjaro*, Volume XII of *Empire Survey Review*, pp. 194–206. Crown Agents' for Overseas Governments and Administration.

Rusu, R. B. and S. Cousins (2011, May 9-13). 3D is here: Point Cloud Library (PCL). In *IEEE International Conference on Robotics and Automation (ICRA)*, Shanghai, China, pp. 1–4.

Saburi, J., N. Angelakis, R. Jaeger, M. Illner, P. Jackson, and K. Pugh (2000, October). Height measurement of Kilimanjaro. *Survey Review 35*(278), 552–562.

Shirima, S. (2013, September 25). personal communication.

Sirguey, P. J., N. J. Cullen, T. Mölg, and G. Kaser (2013, 7-13 December). Ice volume assessment of the northern ice field of kilimanjaro: the photogrammetry strikes back. In *Proceedings of the American Geophysical Union (AGU) fall meeting*, San Francisco, CA, USA, pp. C42A–05. AGU.

Young, J. A. T. and S. Hastenrath (1987). *Glaciers of the Middle East and Africa - Glaciers of Africa* (Richard S. Williams and Jane G. Ferrigno ed.)., pp. G49–G70. Satellite image atlas of glaciers of the World. U.S. Geological Survey.